Frontiers in Health InformaticsISSN-Online: 2676-7104 www.healthinformaticsjournal.com
2024; Vol 13: Issue 3 Open Access

Evaluation of the Usefulness of Self-Made Filters Using 3D Printing Technology in Shoulder Superoinferior Axial Projection

Joo Young-Cheol[1] and Hong Dong-Hee[2*]
[1]Department of Radiology, Samsung Medical Center
[2]Department of Radiological Science, Shinhan University
Corresponding author: Hong Dong-Hee
hansound2@shinhan.ac.kr

Cite this paper as: Joo Young-Cheol and Hong Dong-Hee (2024). Evaluation of the Usefulness of Self-Made Filters Using 3D Printing Technology in Shoulder Superoinferior Axial Projection. *Frontiers in Health Informatics,* 13(3), 4375-4382

ABSTRACT

Purpose: *The purpose of this study is to find out the adjacent organ shielding effect of self-made filters with 3D printing technology and to identify the thickness of the filter for shielding effects similar to bismuth during the shoulder superoinferior axial projection.*

Materials and Methods: *This study used a GC 85A (Samsung Electronics, Korea) X-ray equipment and was conducted on a phantom PBU-60 (Kyotokagaku, Japan) model. The filter production was modeled using the Autodesk fusion 360 program followed by 3D printing using an S3 (Ultimaker, Netherlands) 3D printer, with polylactic acid (Ultimaker, Netherlands) used as the raw material and printed using the fused filament fabrication method. For the shape of the filter, a base and six individual filters (Layer 1–6) that can be attached to the base were produced. The experimental method obtained an image by attaching the base part to the collimator and stacking individual filters up to six layers. Data were obtained 20 times for each group. The exposure parameters were fixed at a tube voltage of 68 kVp, a tube current of 16 ㎃s, an irradiation field of 8" × 10", and a source to image distance of 100 ㎝. In order to measure the entrance skin dose (ESD), the dosimeter element was attached to the breast and thyroid areas.*

Results: *As a result of measuring the average value of the ESD of the breast and thyroid gland according to the change in filter thickness, the non-filter status was 276.39 μGy and 357.77 μGy, and 140.29 μGy and 175.79 μGy, respectively, when bismuth was attached. ESD values measured in the base of the filter were 217.69 μGy and 281.46 μGy, while Layer 1, Layer 2, Layer 3, Layer 4, Layer 5, and Layer 6 measured 180.71 μGy and 233.74 μGy, 150.27 μGy and 185.82 μGy, 127.37 μGy and 166.72 μGy, 112.11 μGy and 143.74 μGy, 94.63 μGy and 121.89 μGy, and 84.72 μGy and 106.71 μGy, respectively.*

Conclusion: *As a result of this study, the average value of ESD decreased by 49% and 50% in breast and thyroid, respectively, compared to the non-filter state. Dose reduction effect was similar to that of bismuth in Layer 2 (45% breast and 48% thyroid) and Layer 3 (53% breast and 53% thyroid). Therefore, a thickness ranging between the thickness of Layer 2 and 3 (3.5 ㎝ in the elbow area, 1.5 ㎝ in the axillary area and 2.5 ㎝ in the chest area) was considered optimal thickness of the 3D-printed filter for efficient shielding of the thyroid and breast.*

Keywords – *3D Printing, Radiography of shoulder joint, Shielding, Bismuth, Entrance Skin Dose (ESD).*

Ⅰ. INTRODUCTION

According to the Healthcare Big Data Open System, the number of patients visiting medical institutions owing to shoulder lesions have increased by approximately 7.6% from 2,268,852 in 2018 to 2,441,837 in 2022 [1]. Basic radiographic examination methods for diagnosing shoulder lesions include anteroposterior, lateral,

anterior-posterior, and posterior-anterior oblique projections of the shoulder joint.

To diagnose shoulder injuries and shoulder joint dislocations, examinations that allow observation of the axillary region must be performed. Representative methods include shoulder superoinferior axial projection and the Lawrence, Westpoint, and Stryker notch methods [2]. However, the Lawrence and Westpoint methods require the patient to be examined in the supine or prone position, which can be a limitation in terms of posture. Whereas, the Stryker notch method, is primarily used to observe the posterolateral aspect of the humeral head, and its purpose differs from the others. In contrast, the shoulder superoinferior axial projection has the advantage of being less restrictive in terms of posture. However, because the body must lean laterally to position the shoulder joint at the center of the image receptor (IR), unnecessary radiation exposure to areas other than the shoulder can occur. Among the exposed areas, the breast and thyroid are organs that are highly sensitive to radiation and require protection from exposure [3,4].

Shielding methods typically involve the use of lead (Pb)- or bismuth-based shields or collimation functionality [5]. However, collimation has a lower shielding rate than Pb shielding, and excessive adjustment can result in incomplete coverage of the target area[6]. Pb is the most commonly used material in clinical practice because of its excellent shielding capabilities and workability. However, it is classified as a heavy metal and poses health risks owing to occupational exposure and absorption into the body[5,7]. In contrast, Bismuth (Bi), has been reported in various studies as a material that can effectively shield radiation due to its excellent dose reduction effects, good workability, and physical flexibility[5,8]. However, it was found that in certain energy settings, Bi had a lower shielding rate relative to its weight than Pb, and it was predicted that there may be limits to weight reduction when commercialized under the same shielding conditions [9].

The 3D printing technology has the advantage of allowing the production of customized medical products and equipment quickly and economically within a few hours. It has been applied in various medical fields in recent years [10]. Related studies are underway on the application of 3D printing technology in radiological examinations and other medical procedures, such as manufacturing shields for patient protection during interventional procedures and shielding lenses during brain CT examinations. However, there is a lack of research on its application in shoulder superoinferior axial projection examinations [11,12].

Therefore, this study aimed to compare the effects of a 3D-printed filter designed for use in shoulder superoinferior axial projection examinations with those of Bi, a radiation-shielding material, on the dose and image quality of the breast, thyroid, and axillary regions. This study aims to present the optimal thickness that can achieve the most similar effect to that of Bi shielding.

Ⅱ. MATERIALS AND METHODS

1. Experimental Subjects

In this study, a human body model phantom, PBU-60 (Kyotokagaku, Japan) and a GC 85A (Samsung Electronics, Korea) X-ray generator were used. The entrance surface dose (ESD) was measured using an Unfors patient skin dosimeter (Unfors Instruments Inc., New Milford, USA).

2. Experimental Methods

1) Filter Manufacturing Process

The process of creating a filter using 3D printing to minimize the heel effect and unnecessary radiation exposure to the breast and thyroid areas is as follows: The design was created using Autodesk Fusion 360 in the form of a wedge filter with a thickness of 1 cm attached to a 0.5 cm thick plate, as shown in Fig. 1-(b). Layers 1–6 were designed to increase the thickness by 1 cm at both ends and 0.5 cm in the concave middle section, as shown in Fig. 1(c). The final filter is modeled as shown in Fig. 1(a). The modeled file was converted into an STL file and processed by 3D slicing (LUGO CURA) using the Fused Filament Fabrication (FFF) method. The filters were printed using a 3D printer (S3, Ultimaker, Netherlands). Polylactic Acid (PLA) was used as the material. Once printed, the filter was separated from the bed and the support structures were removed to complete the filter.

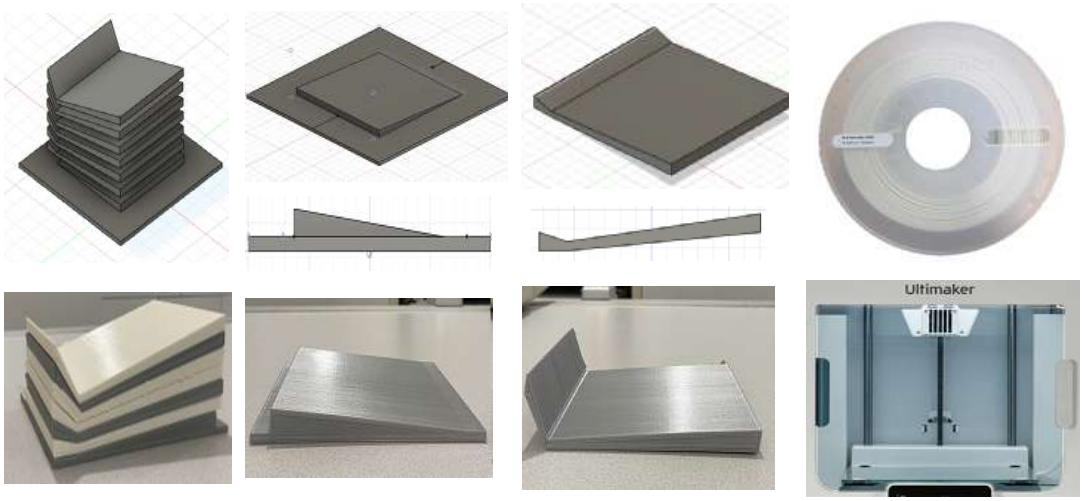

(a) (b) (c) (d)

Fig 1. Description of the filter production method

(a) The entire layer of the filter; (b) 'Base'of the filter; (c) 'Layer 1'of the filter; and (d) shows the 3D printer used to produce the filter and the PLA filament, the material. Polylactic Acid; PLA

2) IMAGE ACQUISITION METHOD

The examination posture was set as shown in Fig. 2(a), with the phantom placed at the edge of the examination table. The left elbow was bent at a right angle and the shoulder joint was tilted to align with the center of the IR surface. The phantom was secured using fixation tools to minimize movement.

In this study, the condition without applying the filter was referred to as "Non-Filter." The custom-made filters were attached to the collimator layer by layer, in sequential order, named "Base," "Layer 1," "Layer 2," "Layer 3," "Layer 4," "Layer 5," and "Layer 6." The comparison case, where only the 1 mm thick Bi shield was attached, was referred to as "Bismuth." Images were acquired for three conditions. First, an image was obtained under the "Non-Filter" condition. Second, images were acquired sequentially by layering a custom-made filter from the Base to Layer 6 on the X-ray collimator, as shown in Fig. 2(b). Third, the images were obtained using an attached Bi shield. For each condition, 20 data sets were collected.

The exposure conditions were fixed at 68 kVp tube voltage, 16 mAs tube current, an irradiation field size of 8" × 10", and a source to image distance (SID) of 100 cm.

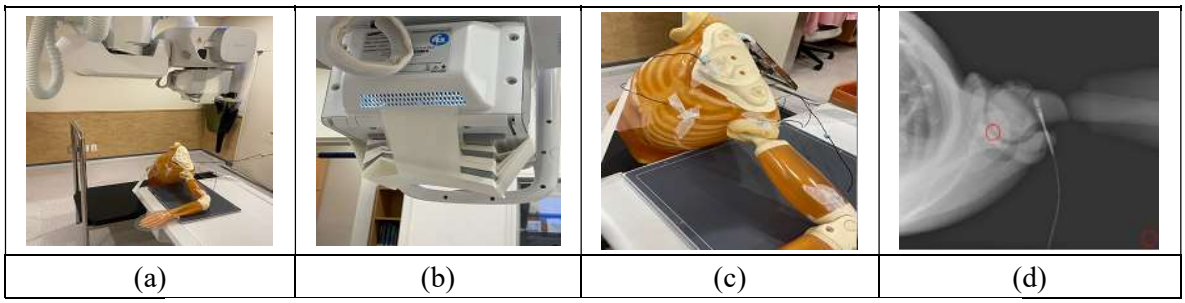

(a) (b) (c) (d)

Fig 2: Description of the experimental method and measurement method

(a) Shows the acquisition of shoulder superoinferior axial projection. (b) Attachment of 3D filters (c) Location of dosimeter element. (d) CNR measurements of evaluation point in shoulder superoinferior axial image. Contrast-to-noise ratio; CNR

3) DOSE MEASUREMENT METHOD

Dosimeter sensors were attached to the chest, neck, and upper shoulder of the phantom to measure the ESDs of the breast, thyroid, and axillary regions, respectively, as shown in Fig. 2(c). Doses in each region were measured simultaneously.

4) IMAGE QUALITY EVALUATION METHOD

In this study, regions of interest (ROI) were set in the background and glenohumeral joint of the acquired images using the Image J program (National Institutes of Health, USA), as shown in Fig. 2(d). The mean value and standard deviation of the pixel signal intensity within the ROI were measured. The mean value and standard deviation of the background signal intensity were calculated, and the contrast-to-noise ratio (CNR) was determined using the following equation (1):

$$\mathrm{CNR} = \left| \frac{(\text{Background SI}_{\text{Avg}} - \text{ROI SI}_{\text{Avg}})}{\sqrt{\text{Background SD}^2 + \text{ROI SD}^2}} \right| \quad \text{Equation (1)}$$

5) DATA ANALYSIS METHOD

In this study, the data measured under each condition were tested for normality using the Shapiro-Wilk test ($p > 0.05$). One-way analysis of variance (ANOVA) was performed to compare the means of each condition. *Post-hoc* testing was conducted using Tukey's method. Statistical analyses were performed using SPSS (version 22.0; SPSS, Chicago, IL, USA). The significance level (α) was set at 0.05, and a p-value of 0.05 or less was considered statistically significant.

Ⅲ. RESULTS

1. Comparison of ESD by Condition for the Breast Region

The average ESD measured in the breast was 276.39 ± 1.12 μGy and 140.29 ± 0.95 μGy for the for the Non-Filter and Bismuth conditions, respectively. For the Base, the ESD was 217.69 ± 0.88 μGy, while Layer 1, Layer 2, Layer 3, Layer 4, Layer 5 and Layer 6 measured 180.71 ± 1.01 μGy, 150.27 ± 0.76 μGy, 127.37 ± 1.09 μGy, 112.11 ± 0.60 μGy, 94.63 ± 0.54 μGy, and 84.72 ± 0.54 μGy, respectively. The mean values for each group were statistically significant ($p < 0.01$), and *post-hoc* analysis showed that all groups were independent of each other (Table 1).

Table 1: Results of the dose comparison of the breast according to the filter

Filter	n	mean ± SD(μGy)	min	max	F	p
Non-Filter	20	276.39 ± 1.12^{i}	274.80	279.20	103368.298	0.01
Bismuth		140.29 ± 0.95^{e}	138.40	142.90		
Base		217.69 ± 0.88^{h}	214.90	219.30		
Layer 1		180.71 ± 1.01^{g}	179.40	182.90		
Layer 2		150.27 ± 0.76^{f}	148.90	151.90		
Layer 3		127.37 ± 1.09^{d}	123.90	128.90		
Layer 4		112.11 ± 0.60^{c}	111.20	113.80		
Layer 5		94.63 ± 0.54^{b}	93.45	95.54		
Layer 6		84.72 ± 0.54^{a}	83.63	85.45		

2. Comparison of ESD by Condition for the Thyroid Region

The average ESD measured for the thyroid was 357.77 ± 1.91 μSv for the Non-Filter condition and 175.79 ± 0.95 μGy for the Bismuth condition. For the Base, the ESD was 281.46 ± 1.10 μGy, while Layer 1, Layer 2, Layer 3, Layer 4, Layer 5, and Layer 6 measured 233.74 ± 1.10 μGy, 185.82 ± 39.14 μGy, 166.72 ± 1.52 μGy, 121.90 ± 0.88 μGy, 21.89 ± 0.88 μGy, and 106.71 ± 0.56 μGy, respectively, showing differences between each

condition. The mean values for each group were statistically significant ($p < 0.01$), and the *post-hoc* analysis indicated that each group was independent (Table 2).

Table 2: Results of the dose comparison of the thyroid according to the filter

Filter	n	mean ± SD(μGy)	min	max	F	p
Non-Filter	20	357.77 ± 1.91[i]	354.80	362.20	764.816	0.01
Bismuth		175.79 ± 0.95[e]	174.80	178.70		
Base		281.46 ± 1.10[h]	278.90	284.10		
Layer 1		233.74 ± 1.10[g]	232.40	236.40		
Layer 2		185.82 ± 1.14[f]	183.57	188.80		
Layer 3		166.72 ± 1.52[d]	161.60	169.00		
Layer 4		143.74 ± 0.69[c]	143.41	144.06		
Layer 5		121.89 ± 0.88[b]	118.80	123.30		
Layer 6		106.71 ± 0.56[a]	105.70	107.60		

3. Comparison of ESD by Condition for the Axillary Region

The average ESD measured for the axillary region was 385.65 ± 2.06 μGy for the Non-Filter condition and 183.58 ± 0.96 μGy for the Bismuth condition, as shown in Table 3. For the Base, the ESD was 285.94 ± 0.86 μGy, while Layer 1, Layer 2, Layer 3, Layer 4, Layer 5, and Layer 6 measured 230.94 ± 0.86 μGy, 185.29 ± 0.77 μGy, 152.54 ± 1.29 μGy, 132.30 ± 0.55 μGy, 106.67 ± 0.93 μGy, and 94.26 ± 0.60 μGy, respectively. The mean values for each group were statistically significant ($p < 0.01$), and *post-hoc* analysis indicated that each group was independent.

Table 3: Results of the dose comparison of the axillary region according to the filter

Filter	n	mean ± SD(μGy)	min	max	F	p
Non-Filter	20	385.65 ± 2.06[i]	384.68	386.60	143359.575	0.01
Bismuth		183.58 ± 0.96[e]	183.13	184.02		
Base		285.94 ± 0.86[h]	284.00	287.50		
Layer 1		230.28 ± 1.12[g]	228.70	232.80		
Layer 2		185.29 ± 0.77[f]	183.80	186.80		
Layer 3		152.54 ± 1.29[d]	148.20	154.20		
Layer 4		132.30 ± 0.55[c]	131.20	133.20		
Layer 5		106.67 ± 0.93[b]	104.00	108.60		
Layer 6		94.26 ± 0.60[a]	93.29	95.90		

4. Comparison of CNR for the Glenohumeral Joint by Filter Thickness Variation

The average CNR measured for the glenohumeral joint was 11.97 ± 0.17 μGy for the Non-Filter condition and 12.13 ± 0.05 μGy for the Bismuth condition, as shown in Table 4. For the Base, the CNR was 13.95 ± 0.07 μGy, while Layer 1, Layer 2, Layer 3, Layer 4, Layer 5, and Layer 6 measured 24.17 ± 0.14 μGy, 19.33 ± 0.12 μGy, 13.39 ± 0.12 μGy, 15.66 ± 0.11 μGy, 12.92 ± 0.40 μGy, and 11.44 ± 0.05 μGy, respectively. The mean values for each group were statistically significant ($p < 0.01$), and the *post-hoc* analysis indicated that each group was independent of the others.

Table 4: CNR results according to image quality of the glenohumeral joint

Filter	n	mean ± SD(μGy)	min	max	F	p
Non-Filter	20	11.97 ± 0.17[h]	12.62	11.76	12229.24	0.01
Bismuth		12.13 ± 0.05[g]	12.27	12.01		
Base		13.95 ± 0.07[e]	14.09	13.83		
Layer 1		24.17 ± 0.14[a]	24.42	23.82		
Layer 2		19.33 ± 0.12[b]	19.54	19.07		
Layer 3		18.39 ± 0.12[c]	18.65	18.15		
Layer 4		15.66 ± 0.11[d]	15.82	15.40		
Layer 5		12.92 ± 0.40[f]	14.58	12.64		
Layer 6		11.44 ± 0.05[i]	11.55	11.36		

Ⅳ. DISCUSSION

The radiation protection goal proposed by the International Commission on Radiological Protection (ICRP) is to "prevent the occurrence of deterministic effects due to radiation exposure and to keep stochastic effects as low as reasonably achievable." Among the various methods used to shield against exposure outside the intended examination area, the most commonly used is the protective Pb shielding. However, Pb can obscure the anatomical structures in images and create artifacts. To address this, various studies have been conducted on the production of shielding materials using 3D printing. Previous studies have shown that 3D-printed shields made of PLA exhibit a reduction effect ranging from 5.2%–27.4% in breast exposure during abdominal examinations, depending on their thickness. Studies using mixtures of Al, Bi, Cu, Fe, W, and stainless steel with PLA and Acrylonitrile Butadiene Styrene (ABS) have reported the highest shielding rates with combinations of ABS + W, PLA + Stainless steel, and ABS + Bi. Although 3D printing technology using additive manufacturing methods has been actively researched, studies specifically applying the related additional filters are still lacking. This study aimed to compare the average ESD values of a filter made of PLA using 3D printing with aBi shield during shoulder superoinferior axial projection examination, presenting a thickness that can achieve similar effects. These results can serve as foundational data for the production of additional X-ray filters using 3D printing.

According to the results of this study, the average ESD values decreased by 49.24%, 50.8%, and 52.39% for the breast, thyroid, and axillary regions, respectively, compared with the Non-Filter condition with the bismuth shield. When comparing Non-Filter with Layer 2 and Layer 3, a decrease of 45.63% and 53.91% was observed for the breast, 48.06% and 53.4% for the thyroid, and 51.95% and 60.4% for the axillary regions, respectively. The average CNR values measured for image quality evaluation increased compared to the Non-Filter and Bismuth conditions, except for Layer 6, suggesting that it could contribute to reducing the patient exposure dose without degrading image quality. However, the CNR value significantly increased in Layer 1, but then sharply decreased in Layer 2. The cause of this phenomenon is not yet clearly understood and requires further investigation.

Application of the self-manufactured filter during shoulder superoinferior axial projection examination confirmed a reduction in the exposure dose to the breast and thyroid gland. The thickness at the elbow (3.5–4.5 cm), axillary (1.5–2 cm), and chest area (2.5–3.5 cm) ranging between Layer 2 and Layer 3 showed results similar to the shielding effectiveness of Bi.

This study utilized only PLA as the 3D printing material and was conducted on a phantom model. Thus, further research using various materials while considering human applications is necessary.

Ⅳ. CONCLUSION

This study aimed to apply a self-manufactured filter using 3D printing technology during shoulder superoinferior axial projection examination, and to compare the dose and image quality of the breast, thyroid, and axillary regions with those of Bi, ultimately identifying a thickness that could yield similar effects.

The results indicated that the respective thickness of the filter 3.5–4.5 cm, 1.5–2 cm, and 2.5–3.5 cm at the

elbow, axillary region, and chest area provided results similar to the shielding effectiveness of Bi (49.24% for the breast, 50.8% for the thyroid, and 52.39% for the axillary region), confirming the utility of filters between Layer 2 and Layer 3. The CNR for the glenohumeral joint was higher than the Non-Filter and Bismuth conditions, except for Layer 6.

If appropriately utilized, the 3D-printed filter during shoulder superoinferior axial projection examination could contribute to reducing the dose values for the breast, thyroid, and axillary regions, ultimately decreasing patient exposure.

REFERENCE

1. https://opendata.hira.or.kr/op/opc/olap3thDsInfoTab1.do
2. CKPub. TEXTBOOK of Radiographic positioning and Clinical Diagnosis. 3rd ed. vol. 2. Medical Imaging Technology Research Association; 2008.
3. Kazuki Takegami, Hiroaki Hayashi, Tatsuya Maeda. Thyroid dose reduction shield with the generation of less artifacts used for fast chest CT examination. Radiation Physics and chemistry Volume 203, Part B, February 2023, 110635
4. Cécile M Ronckers, Christine A Erdmann, Charles E Land. Radiation and breast cancer: a review of current evidence. Breast Cancer Res. 2005; 7(1): 21–32. Published online 2004 Nov 23. doi: 10.1186/bcr970
5. Mansour Zabihzadeh, Mehrdad Gholami. Dose Reduction to the Thyroid Gland in Pediatric Chest Radiography. International Journal of Pediatrics. 2016
6. Servaes S, Zhu X. The effects of bismuth breast shields in conjunction with automatic tube current modulation in CT imaging. Pediatric Radiology. 2013; 43(10):1287-94.
7. Raissaki M, Perisinakis, K, Damilakis J, Nicholas G. Eye-lens bismuth shielding in paediatric head CT: artefact evaluation and reduction. Pediatric Radiology. 2010; 40(11):1748-54.
8. Singh B, Chandran V, Bandhu HK, et al. Impact of lead exposure on pituitary-thyroid axis in humans. Biometals. 2000;13(2):187-92.
9. Hoon-Hee Park. The Evaluation of Performance and Usability of Bismuth, Tungsten Based Shields
10. Ventola, C.L. Medical Applications for 3D Printing: Current and Projected Uses. P T Peer-Rev. J. Formul. Manag. 2014; 39, 704–711. [Google Scholar]
11. Cho Yong-In. Feasibility of the 3D Printing Materials for Radiation Dose Reduction in Interventional Radiology. Journal of Radiological Science and Technology, 43(3), 169-176
12. Woo Jeon Choi, Dong Hyun Kim. A Study on the Shielding of Orbit by 3D Printed Filament in Brain CT. J. Korean Soc. Radiol., Vol. 15, No. 2. 21, April 2021
13. Ki-Won Kim, Jung-Whan Min1, Kwang-Yeul Lyu1. Comparison Study on CNR and SNR of Thoracic Spine Lateral Radiography. Comparison Study on CNR and SNR of Thoracic Spine Lateral Radiography. J. Korean Soc. Radiol., Vol. 36, No. 4, 2013
14. https://www.kdca.go.kr/contents.es?mid=a20305010000
15. Yong In Cho, Jung Hoon Kim. Evaluation of the Effectiveness of 3D Printing Shielding Devices using Monte Carlo Simulation in Plain Radiography. J. Korean Soc. Radiol., Vol. 14, No. 3, June 2020
16. Lee WH, Ahn SM. Evaluation of Reductive Effect of Exposure Dose by Using Air Gap Apron in Nuclear Medicine Related Work Environment. The Journal of the Korea Contents Association. 2014;14(12): 845-53.

17. Gang HH, Kim DH. A Study on Barium Mixed Radiation Shield using 3D printer. J. Korean Soc. Radiol. 2020;14(5):627-34.